J|A|C|S ARTICLES

Published on Web 09/21/2010

Multiple Release Kinetics of Targeted Drug from Gold Nanorod Embedded Polyelectrolyte Conjugates Induced by Near-Infrared Laser Irradiation

Tsung-Rong Kuo,[†] Vladimir A. Hovhannisyan,[‡] Yu-Ching Chao,[†] Shu-Ling Chao,[†] Shu-Jen Chiang,[§] Sung-Jan Lin,[||,⊥] Chen-Yuan Dong,[‡] and Chia-Chun Chen*[,†,§]

Department of Chemistry, National Taiwan Normal University, Taipei 116, Taiwan, Department of Physics, National Taiwan University, Taipei 106, Taiwan, Institute of Atomic and Molecular Sciences, Academia Sinica, Taipei 106, Taiwan, Institute of Biomedical Engineering, College of Medicine and College of Engineering, National Taiwan University, Taipei 106, Taiwan, and Department of Dermatology, National Taiwan University Hospital and College of Medicine, Taipei 106, Taiwan

Received June 18, 2010; E-mail: cjchen@ntnu.edu.tw

Abstract: The conjugates of gold nanorods and the model drug, fluorescein isothiocyanate (FITC), embedded inside polyelectrolytes (GNRs/FITC@PLE) were synthesized to study the release kinetics of FITC under femtosecond near-infrared (NIR) laser irradiation. The optical and structural properties of GNRs/FITC@PLE conjugates before and after laser treatments were examined using UV−vis spectroscopy, confocal microscopy, and transmission electron microscopy (TEM). The release of FITC from the conjugates was induced by the heat generated from gold nanorods under laser irradiation. The concentration of released FITC was measured as the time of continuous and periodic laser irradiation was varied. Within 5 min of the laser exposure, the release rates of FITC exhibited zero-order and first-order kinetics under continuous and periodic irradiation, respectively. Furthermore, a drug release system was designed based on the conjugates of gold nanorods and the anticancer drug, paclitaxel (PTX), embedded inside polyelectrolytes (GNRs/PTX@PLE). The conjugates were applied for in vitro studies with breast cancer cells. The release of PTX from the conjugates was triggered by NIR laser irradiation, and the inhibition rates of the cells showed strong dependencies on the irradiation modes and time. The results suggested that the multiple releases of PTX from the conjugates can be controlled by laser irradiation within a long period of time. Our system holds great potential for future therapeutic applications on breast cancers.

Introduction

The development of new materials for drug delivery systems has become one of the most important tasks in the studies of pharmacokinetics.[1−7] Recent advances have been focused on the designs of inorganic nanomaterials as a new drug carrier.[8−15] Different types of nanomaterials such as mesoporous silica, carbon nanotubes, porous silicon, and gold nanoparticles were developed as drug releasing systems. Vancomycins were stored and released from the pore voids of SBA-15 silica rods in a pH-value-dependent fashion.[16] Carbon nanotubes were used as an effective drug carrier to conjugate with platinum(IV) anticancer drug.[17] For controlled delivery of the anticancer agent doxorubicin, porous silicon was covered with a stamped biodegradable material in creating a continuous drug release platform.[18] Gold nanoparticles, nanorods and nanocages were conjugated with targeted drugs to enhance the delivery efficiency

[†] National Taiwan Normal University.
[‡] Department of Physics, National Taiwan University.
[§] Academia Sinica.
[||] Institute of Biomedical Engineering, National Taiwan University.
[⊥] National Taiwan University Hospital and College of Medicine.

(1) LaVan, D. A.; McGuire, T.; Langer, R. *Nat. Biotechnol.* **2003**, *21*, 1184–1191.
(2) Allen, T. M.; Cullis, P. R. *Science* **2004**, *303*, 1818–1822.
(3) Sengupta, S.; Eavarone, D.; Capila, I.; Zhao, G.; Watson, N.; Kiziltepe, T.; Sasisekharan, R. *Nature* **2005**, *436*, 568–572.
(4) Horcajada, P.; Serre, C.; Maurin, G.; Ramsahye, N. A.; Balas, F.; Vallet-Regí, M. a.; Sebban, M.; Taulelle, F.; Férey, G. r. *J. Am. Chem. Soc.* **2008**, *130*, 6774–6780.
(5) Pan, D.; Caruthers, S. D.; Hu, G.; Senpan, A.; Scott, M. J.; Gaffney, P. J.; Wickline, S. A.; Lanza, G. M. *J. Am. Chem. Soc.* **2008**, *130*, 9186–9187.
(6) Rieter, W. J.; Pott, K. M.; Taylor, K. M. L.; Lin, W. *J. Am. Chem. Soc.* **2008**, *130*, 11584–11585.
(7) Cu, Y.; Saltzman, W. M. *Nat. Mater.* **2009**, *8*, 11–13.
(8) Ziaie, B.; Baldia, A.; Leia, M.; Guc, Y.; Siegelb, R. A. *Adv. Drug Delivery Rev.* **2004**, *56*, 145–172.
(9) Soppimath, K. S.; Tan, D. C.-W.; Yang, Y.-Y. *Adv. Mater.* **2005**, *17*, 318–323.
(10) Kim, H. J.; Matsuda, H.; Zhou, H.; Honma, I. *Adv. Mater.* **2006**, *18*, 3083–3088.
(11) Park, H.; Yang, J.; Seo, S.; Kim, K.; Suh, J.; Kim, D.; Haam, S.; Yoo, K. H. *Small* **2008**, *4*, 192–196.
(12) Kim, J.; Lee, J. E.; Lee, S. H.; Yu, J. H.; Lee, J. H.; Park, T. G.; Hyeon, T. *Adv. Mater.* **2008**, *20*, 478–483.
(13) Liong, M.; Lu, J.; Kovochich, M.; Xia, T.; Ruehm, S. G.; Nel, A. E.; Tamanoi, F.; Zink, J. I. *ACS Nano* **2008**, *2*, 889–896.
(14) Cheng, Y.; Samia, A. C.; Meyers, J. D.; Panagopoulos, I.; Fei, B.; Burda, C. *J. Am. Chem. Soc.* **2008**, *130*, 10643–10647.
(15) Chen, J.; Chen, S.; Zhao, X.; Kuznetsova, L. V.; Wong, S. S.; Ojima, I. *J. Am. Chem. Soc.* **2008**, *130*, 16778–16785.
(16) Yang, Q.; Wang, S.; Fan, P.; Wang, L.; Di, Y.; Lin, K.; Xiao, F. S. *Chem. Mater.* **2005**, *17*, 5999–6003.
(17) Feazell, R. P.; Nakayama-Ratchford, N.; Dai, H.; Lippard, S. J. *J. Am. Chem. Soc.* **2007**, *129*, 8438–8439.

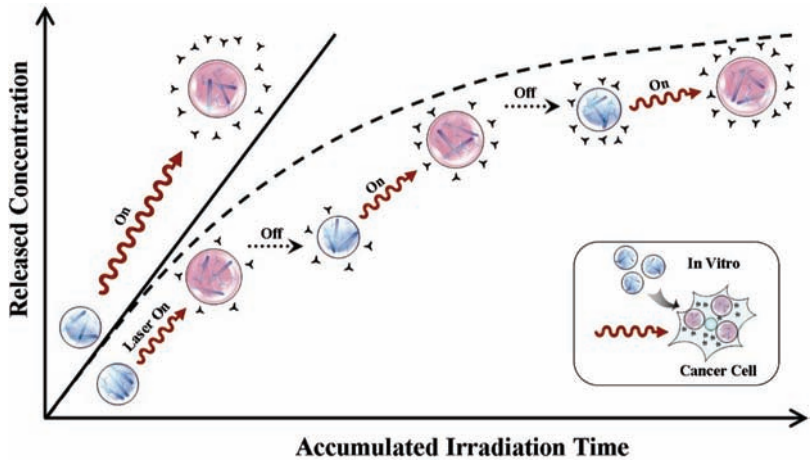

Figure 1. Schematic illustration of multiple releases of model drug from gold nanorod embedded polyelectrolytes under NIR laser irradiation. The release of the model drug from the conjugates is described while the conjugates are irradiated by the laser continuously (laser on and off for one time) or periodically (laser on and off alternatively for two or three times). The linear and exponential curves in the plot of accumulated irradiation time versus released model drug concentration demonstrate different release kinetics behaviors under continuous and periodic laser irradiations. The schematic illustration (inset) shows that the inhibition rates of cancer cells are measured after the conjugates entered the cells and the release of the drug from the conjugates is triggered by the laser.

under optically induced release.[19−21] In these approaches, the unique structural properties of nanomaterials of a high surface to volume ratio and hollow structure provided significant advantages in the design of efficient drug carriers. More importantly, nanomaterials with specific optical or magnetic characteristics may also be used as a new triggering system for the controlled release of targeted drug molecules.

Previous studies have shown that the magnetic and gold nanoparticles can be used as controlled release carriers for drug molecules under the respective application of an oscillating magnetic field and optical illumination.[22−25] In the presence of an oscillating external magnetic field, superparamagnetic nickel ferrite nanoparticles conjugated with a polymethacrylic acid polymer and the anticancer drug doxorubicin were shown to result in a significant enhancement of drug release efficiency.[26] The enhancement was largely due to compressive and tensile stresses of the nanoparticle deformation by the magnetic field. Other than the use of magnetic field, ultraviolet and NIR light irradiation have also been used to induce drug release from the conjugates of gold nanoparticles and liposomes.[27−30] The release of the drug from the conjugates was mainly caused by a morphological change of the conjugates induced by the conversion of the absorbed energy into heat. The success of these methods in controlling drug release has motivated the designs of new drug releasing systems based on nanomaterials.

Several studies have used gold nanorods as carriers in the conjugates of biomolecules such as DNA and drugs for photoactivated release of these biomolecules.[31−33] Gold nanorods can be heated to high temperature by pulsed NIR laser excitation of their longitudinal surface plasmon resonance.[34−37] The heat was accumulated on gold nanorods between 10 and 50 ps and then dissipated to the surroundings within approximately 100 ps to 1 ns.[38] The rapid heat accumulation (on) and dissipation (off) of the nanorods under NIR laser irradiation have been utilized to design several new biomolecule releasing systems.[20,32,39] For clinical applications, gold nanorods are known to be of lower cytotoxicity in comparison to other inorganic nanomaterials.[40−43] Furthermore, deeper tissue penetration and reduction in photodamage can be achieved when NIR laser irradiation is executed in inducing drug release from gold nanorod conjugates.[44,45] These studies suggest that a novel drug releasing system may be possibly designed by using gold nanorods as the carrier and that the concentration of released drug can be adjusted by control of the external laser power, frequencies, and exposure time.

In this work, we have synthesized and characterized the conjugates of gold nanorods and the model drug, FITC,

(18) Vaccari, L.; Canton, D.; Zaffaroni, N.; Villa, R.; Tormen, M.; Fabrizio, E. d. *Microelectron. Eng.* **2006**, *83*, 1598–1601.
(19) Podsiadlo, P.; Sinani, V. A.; Bahng, J. H.; Kam, N. W. S.; Lee, J.; Kotov, N. A. *Langmuir* **2008**, *24*, 568–574.
(20) Shiotani, A.; Mori, T.; Niidome, T.; Niidome, Y.; Katayama, Y. *Langmuir* **2007**, *23*, 4012–4018.
(21) Yavuz, M. S.; Cheng, Y.; Chen, J.; Cobley, C. M.; Zhang, Q.; Rycenga, M.; Xie, J.; Kim, C.; Song, K. H.; Schwartz, A. G.; Wang, L. V.; Xia, Y. *Nat. Mater.* **2009**, *8*, 935–939.
(22) Cao, S.-W.; Zhu, Y.-J. *J. Phys. Chem. C* **2008**, *112*, 12149–12156.
(23) Hu, S.-H.; Liu, T.-Y.; Huang, H.-Y.; Liu, D.-M.; Chen, S.-Y. *Langmuir* **2008**, *24*, 239–244.
(24) Huang, S.; Yang, P.; Cheng, Z.; Li, C.; Fan, Y.; Kong, D.; Lin, J. *J. Phys. Chem. C* **2008**, *112*, 7130–7137.
(25) Zhao, W.; Chen, H.; Li, Y.; Li, L.; Lang, M.; Shi, J. *Adv. Funct. Mater.* **2008**, *18*, 2780–2788.
(26) Rana, S.; Gallo, A.; Srivastava, R. S.; Misra, R. D. K. *Acta Biomater.* **2007**, *3*, 233–242.
(27) Paasonen, L.; Laaksonen, T.; Johans, C.; Yliperttula, M.; Kontturi, K.; Urtti, A. *J. Controlled Release* **2007**, *122*, 86–93.
(28) Troutman, T. S.; Leung, S. J.; Romanowski, M. *Adv. Mater.* **2009**, *21*, 2334–2338.
(29) Volodkin, D. V.; Skirtach, A. G.; Mohwald, H. *Angew. Chem., Int. Ed.* **2009**, *48*, 1807–1809.
(30) Jin, Y.; Gao, X. *J. Am. Chem. Soc.* **2009**, *131*, 17774–17776.
(31) Chen, C. C.; Lin, Y. P.; Wang, C. W.; Tzeng, H. C.; Wu, C. H.; Chen, Y. C.; Chen, C. P.; Chen, L. C.; Wu, Y. C. *J. Am. Chem. Soc.* **2006**, *128*, 3709–3715.
(32) Wijaya, A.; Schaffer, S. B.; Pallares, I. G.; Hamad-Schifferli, K. *ACS Nano* **2009**, *3*, 80–86.
(33) Karg, M.; Pastoriza-Santos, I.; Perez-Juste, J.; Hellweg, T.; Liz-Marzan, M. *Small* **2007**, *3*, 1222–1229.
(34) Link, S.; Burda, C.; Mohamed, M. B.; Nikoobakht, B.; El-Sayed, M. A. *J. Phys. Chem. A* **1999**, *103*, 1165–1170.
(35) Alper, J.; Hamad-Schifferli, K. *Langmuir* **2010**, *26*, 3786–3789.
(36) Norman, R. S.; Stone, J. W.; Gole, A.; Murphy, C. J.; Sabo-Attwood, T. L. *Nano Lett.* **2008**, *8*, 302–306.
(37) Horiguchi, Y.; Honda, K.; Kato, Y.; Nakashima, N.; Niidome, Y. *Langmuir* **2008**, *24*, 12026–12031.
(38) Ekici, O.; Harrison, R. K.; Durr, N. J.; Eversole, D. S.; Lee, M.; Yakar, A. B. *J. Phys. D* **2008**, *41*, 1–11.
(39) Alper, J.; Crespo, M.; Hamad-Schifferli, K. *J. Phys. Chem. C* **2009**, *113*, 5967–5973.

embedded inside polyelectrolytes (GNRs/FITC@PLE). The difference in kinetics behaviors of FITC released from the conjugates was explored when continuous or periodic laser irradiation was applied on the conjugates (Figure 1). Furthermore, a new drug release system was designed based on the conjugates of gold nanorods and the anticancer drug, PTX, embedded inside polyelectrolytes (GNRs/PTX@PLE). The PTX release from the conjugates was triggered by NIR laser irradiation, and in vitro inhibition rate measurements of breast cancer cells were performed as the irradiation modes and time were varied. We believe that the system has provided a new route to control the release of the anticancer drug by laser irradiation for future therapeutic applications.

Experimental Section

Materials. Cetyltrimethylammonium bromide (CTAB, 99+ %), chloroauric acid ($HAuCl_4$ $3H_2O$), L-ascorbic acid (99%), fluorescein isothiocyanate isomer I (FITC, 90%), and silver nitrate (99%) were purchased from Acros. Sodium borohydride (96%) was purchased from Fluka. Poly(acrylic acid) (PAA, M_w ~15000 g/mol) and polydiallyldimethylammonium chloride (PDC, M_w ~15 000 g/mol) were obtained from Aldrich and used without further purification. Dimethyl sulfoxide (DMSO, 99.5%), 3-(4,5-dimethylthiazol-2-yl)-2,5-diphenyltetrazolium bromide (MTT, powder 97.5+ %), and paclitaxel (PTX) were purchased from Sigma.

Synthesis of Gold Nanorods. Water-soluble gold nanorods were synthesized via seed-mediated growth routes according to the literatures.[46] First, the seed solution was prepared as follows: 1 mL of CTAB solution (0.2 M) was mixed with 1 mL of $HAuCl_4$ (0.0005 M). While the solution was stirred at 25 °C, 0.12 mL of ice-cold 0.01 M $NaBH_4$ was added, and the resulting seed solution turned to a brownish yellow color. Second, the growth solution was prepared as follows: 50 mL of $HAuCl_4$ (0.001 M), 50 mL of CTAB (0.2 M), and 2.5 mL of $AgNO_3$ (0.004 M) were mixed at 25 °C. After gentle mixing of the solution, 0.7 mL of ascorbic acid (0.079 M) was added to the solution, and the solution color changed from dark yellow to colorless. To generate gold nanorods, 0.12 mL of the seed solution was added to the growth solution at 27−30 °C under gentle mixing. Within 10−20 min, the combined solution gradually changed to a brownish red color. And then, 1 mL of the brownish red solution was taken in a microcentrifuge tube and centrifuged once at 14 462 *g* for 10 min. A precipitate of gold nanorods was formed at the bottom of the microcentrifuge tube, and the supernatant colorless solution was slowly removed without disturbing the precipitate. For the following experiments, the precipitate of gold nanorods was redispersed in 1 mL of 1 mM NaCl solution. Finally, the sample of gold nanorods was characterized by the TEM (Hitachi H-7100) and UV−vis spectrometer (HP-8453).

Preparation of GNRs/FITC@PAA Conjugates. Stock solution of PAA was prepared in 1 mM aqueous NaCl at 20 mg/mL.[47] Stock solution of FITC was prepared in deionized water at 0.3 mg/mL. Subsequently, the Zetasizer (Malvern Zetasizer 3000 HS) was used to determine the zeta-potential of FITC by the zeta-potential function. The stock solution of FITC was directly measured by the Zetasizer before they were adsorbed onto the gold nanorods. Formulation of GNRs/FITC@PAA conjugates was achieved by alternate adsorption of anionic PAA and cationic FITC upon a net positive charge of CTAB on the gold nanorods surface. First, 200 μL of PAA stock solution were added to the microcentrifuge tube containing 1 mL of the as-prepared gold nanorods solution. After gentle mixing for 30 min, the excess polymer in the supernatant fraction was removed by centrifugation (14 462 *g*, 10 min), and the precipitate of gold nanorods conjugated with PAA was redispersed in 1 mL of 1 mM NaCl solution. Second, 30 μL of FITC stock solution were added to the gold nanorods conjugated with the PAA solution. Subsequently, the PAA conjugated on the gold nanorods surface was adsorbed with FITC for 30 min under gentle mixing and then centrifuged (14 462 *g*, 10 min) to remove the excess FITC in the supernatant. The precipitate of gold nanorods conjugated with PAA and FITC was redispersed in 1 mL of 1 mM NaCl solution. Finally, PAA was conjugated again by repeating the procedure described above. After complete conjugation, the solution containing the GNRs/FITC@PAA conjugate was centrifuged (14 462 *g*, 10 min) once to remove the supernatant. The precipitate of GNRs/FITC@PAA conjugates was redispersed in 1 mL of 1 mM NaCl solution for further experiments.

Preparation of GNRs/PTX@PDC. A stock solution of PTX was prepared in DMSO at 8.7 mg/mL, and PDC was prepared in 1 mM aqueous NaCl at 20 mg/mL. A 5 μL aliquot of PTX stock solution was added to the microcentrifuge tube containing 1 mL of the as-prepared gold nanorods solution. After gentle mixing for 30 min, the excess PTX in the supernatant fraction was removed by centrifugation (14 462 *g*, 10 min), and the precipitate was redispersed in 1 mL of 1 mM NaCl solution. The solution of gold nanorods conjugated with PTX was added with 200 μL of PDC stock solution and then absorbed for 30 min under gentle mixing. After adsorption, the solution containing GNRs/PTX@PDC conjugates was centrifuged (14 462 *g*, 10 min) to remove the excess PDC in the supernatant. The precipitate of GNRs/PTX@PDC conjugates was redispersed in 1 mL of 1 mM NaCl solution for further experiments.

Preparation of GNRs/PAA@PDC. Stock solutions of PAA (20 mg/mL) and PDC (20 mg/mL) were prepared in 1 mL of 1 mM NaCl solution. A 200 μL aliquot of PAA stock solution was added to the microcentrifuge tube containing 1 mL of the as-prepared gold nanorods solution. After gentle mixing for 30 min, the solution was centrifuged (14 462 *g*, 10 min) and supernatant was removed. The precipitate of the gold nanorods conjugated with PAA was redispersed in 1 mL of 1 mM NaCl solution. Afterward, the solution containing gold nanorods conjugated with PAA was added with PDC stock solution (200 μL). After gentle mixing for 30 min, the solution containing gold nanorods conjugated with PAA and PDC was centrifuged (14 462 *g*, 10 min) to remove the excess PDC in the supernatant. The precipitate of GNRs/PAA@PDC conjugates was redispersed in 1 mL of 1 mM NaCl solution for further experiments.

FITC Released from GNRs/FITC@PAA Conjugates Using Femtosecond NIR Laser Irradiation. A diode-pumped solid-state-pumped (Millennia X; Spectra Physics, Mountain View, CA) titanium-sapphire laser (Tsunami; Spectra Physics) capable of producing 80-MHz, femtosecond laser pulses in the spectral range of 700 to 1000 nm was used as the laser source. For our experiments, a titanium-sapphire laser tuned to a wavelength of 775 nm emitting pulses of 120 fs duration was used to irradiate the GNRs/FITC@PAA conjugate solution. A home-built two-photon microscope based on a commercial upright microscope (E800; Nikon, Japan) was used in this study. The output of a titanium-sapphire pulse laser (Tsunami TM, Spectra Physics, Mountain View, CA) pumped by a diode-pumped, solid state laser (Millennia TM X, Spectra Physics, Mountain View, CA) operating at a wavelength of 780 nm was used as the excitation source. The system has already connected with a fluorescence spectrometer and also designed for other experiments. The power of the laser was

(40) Ding, H.; Yong, K. T.; Roy, I.; Pudavar, H. E.; Law, W. C.; Bergey, E. J.; Prasad, P. N. *J. Phys. Chem. C* **2007**, *111*, 12552–12557.
(41) Obare, S. O.; Jana, N. R.; Murphy, C. J. *Nano Lett.* **2001**, *1*, 601–603.
(42) Colvin, V. L. *Nat. Biotechnol.* **2003**, *21*, 1166–1170.
(43) Takahashi, H.; Niidome, Y.; Niidome, T.; Kaneko, K.; Kawasaki, H.; Yamada, S. *Langmuir* **2006**, *22*, 2–5.
(44) Becker, A.; Hessenius, C.; Licha, K.; Ebert, B.; Sukowski, U.; Semmler, W.; Wiedenmann, B.; Grötzinger, C. *Nat. Biotechnol.* **2001**, *19*, 327–331.
(45) Weissleder, R. *Nat. Biotechnol.* **2001**, *19*, 316–317.
(46) Nikoobakht, B.; El-Sayed, M. A. *Chem. Mater.* **2003**, *15*, 1957–1962.
(47) Gole, A.; Murphy, C. J. *Chem. Mater.* **2005**, *17*, 1325–1330.

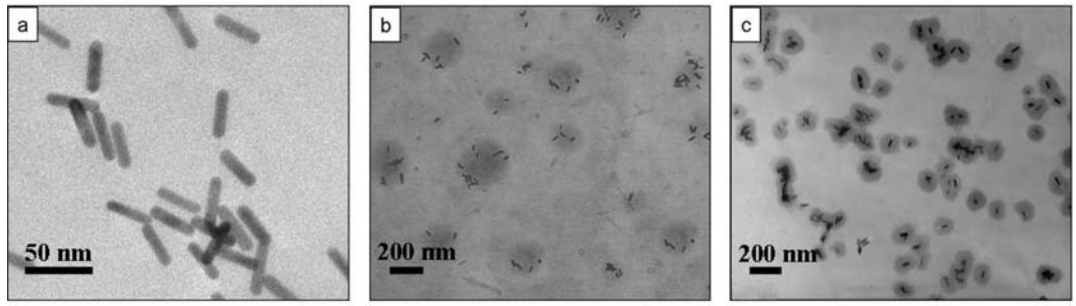

Figure 2. TEM images of (a) gold nanorods and (b) GNRs/FITC@PAA and (c) GNRs/PTX@PDC conjugates before laser irradiation.

1.00 W/cm^2, and the spot size of the laser beam was 2.0 mm. The conjugate solution (1 mL) was irradiated with an NIR laser using a continuous or periodic irradiation mode. In continuous irradiation mode, the NIR laser at 775 nm was applied onto the individual conjugate solution for 1, 2, 3, ..., 6 min. After NIR laser irradiation, the conjugate solution was centrifuged (14 462 *g*, 10 s). The supernatant solution including the released FITC was monitored by multiphoton microscopy utilizing the fluorescence emitting from FITC. In periodic irradiation mode, the conjugate solution was prepared with the same concentration as those samples used above. NIR laser irradiation was periodically projected onto the sample for 1 min with the interval lasting for 1 min, and the whole process was repeated five times. Notice that the fluorescence intensity of FITC released from the conjugates into the solution was measured every min within a total 10 min time course by multiphoton microscopy. After measurement, the fluorescence intensity of released FITC was analyzed by ImageJ software. And then the calculated fluorescence intensity of released FITC was fitted to their calibration curve. The concentration of released FITC was determined by the calculated fluorescence intensity.

Cell Viability Assays of MCF-7 Cells after Incubation with Gold Nanorods or GNRs/PTX@PDC or GNRs/PAA@PDC Conjugates. Human breast cancer cell line MCF-7 was maintained in Dulbecco's Modified Eagle Medium (DMEM) supplemented with 3.7 g/L sodium bicarbonate, 1% penicillin, and 10% fetal bovine serum. The culture was placed in a 37 °C humidified atmosphere with 5% CO_2, and the medium was changed every 3 days. After gold nanorods or gold nanorod conjugates were added into the MCF cells, the cell viability was tested by MTT assay. MCF-7 cells were seeded onto 96-well plates at a density of 5000 cells per well. The plates were then returned to incubators for 12 h of cell attachment. After cell attachment, 1 mL of the as-prepared gold nanorods and its conjugate solutions above were separately centrifuged at 14 462 *g* for 10 min. The precipitates were redispersed in 1 or 10 mL of DMEM. For cell viability assay, each well was added with another 100 μL of DMEM with gold nanorods or gold nanorod conjugates for 24 h. After the removal of DMEM, the cells were then treated with 20 μL of MTT (5 mg/mL in PBS) and incubated for 4 h. The medium was then removed, and the cells were lysed with 100 μL of DMSO. Finally, the absorbance of the purple formazan was recorded at 570 nm.

Cell Viability Assays of MCF-7 Cells Incubated with GNRs/PTX@PDC or GNRs/PAA@PDC Conjugates after NIR Irradiation. MCF-7 cells were seeded onto 96-well plates at a density of 5000 cells/well. The plates were then returned to incubators for 12 h of cell attachment. After cell attachment, 1 mL of as-prepared GNRs/PTX@PDC and GNRs/PAA@PDC conjugate solutions above were individually centrifuged at 14 462 *g* for 10 min. The precipitates were redispersed in 10 mL of DMEM. For inhibition rate assay, each well was added with another 100 μL of DMEM containing conjugates for 24 h. The wells containing cells and conjugates were irradiated with the NIR laser under three different irradiation modes: (I), (II), and (III). The differences among the irradiation modes were described in detail below (also see Figure 7). Finally, after NIR laser irradiation, the cells in the wells were cultured for another 24 h. And then the cell viability of the MCF-7 cells was tested by MTT assay as described above. The inhibition rates of the cells after the whole procedures were finally calculated based on the viability data.

Results and Discussion

Structural Properties of Gold Nanorod Conjugates before and after Laser Irradiation. The average aspect ratio of free gold nanorods was calculated to be ~3.8 (length/diameter = ~42/11 in nm) as shown in Figure 2a before they were embedded in polyelectrolytes. The aspect ratio was found to remain unchanged after gold nanorods were conjugated with polyelectrolytes. The preparation of GNRs/FITC@PAA conjugates was achieved by alternate adsorptions of anionic PAA and the cationic model drug of FITC (the zeta potential is +6.4 mV at pH 6.6) upon a net positive charge of surfactant bilayer CTAB on the surface of gold nanorods. Notice that we have found that the zeta potential of FITC ranged from +10.1 to −22.4 mV at pH 3.61 to 9.54, respectively. The results suggested that FITC with either a positive or negative charge can exist in solution depending on the pH value. The reason for the existence is because the electron pair or charge can be delocalized well in the four aromatic rings of FITC molecule.

After the conjugation, the sizes of GNRs/FITC@PAA conjugates were in the range of 100 to 300 nm as shown in Figure 2b. In addition, the number of gold nanorods in each GNRs/FITC@PAA conjugate was in the range of 7−10 as determined from TEM images. By using the similar synthetic procedures of GNRs/FITC@PAA, GNRs/PTX@PDC conjugates were also prepared by sequential adsorption of the anticancer drug, PTX, and polyelectrolyte PDC. Their sizes were in the range of 100 to 150 nm (Figure 2c), and the number of gold nanorods in each conjugate was approximately 3−5. The average aspect ratio of gold nanorods in the conjugates remained at ~3.8 after the conjugation. Both GNRs/FITC@PAA and GNRs/PTX@PDC conjugates exhibited high solubility in water and in other water-based ionic solutions for further biological tests.

Adjustments of the Power and Time of Laser Irradiation on Gold Nanorod Conjugates Based on UV−vis Spectroscopy and TEM Measurements. Many studies have demonstrated the photothermal conversion effect of gold nanorods by laser irradiation. In our experiments, the adjustment of laser irradiation power and time is the key to delicately inducing the release of the model drug from the conjugates. Here, laser irradiation with the power set at 0.7, 1, and 1.9 W/cm^2 was applied for different time periods (from 10 s to 20 min) to test the stability of GNRs/FITC@PAA conjugates.

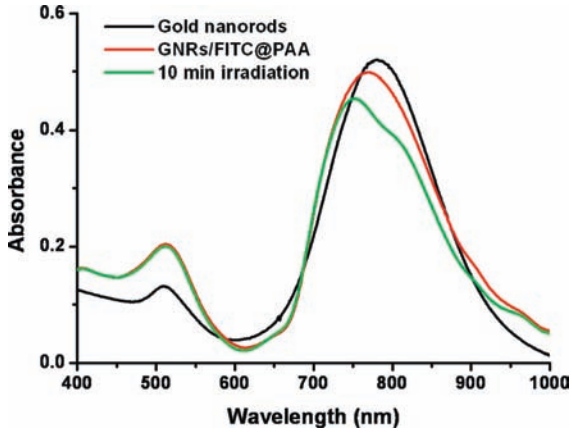

Figure 3. UV−vis spectra of gold nanorods and GNRs/FITC@PAA conjugates before and after irradiation with NIR laser for 10 min.

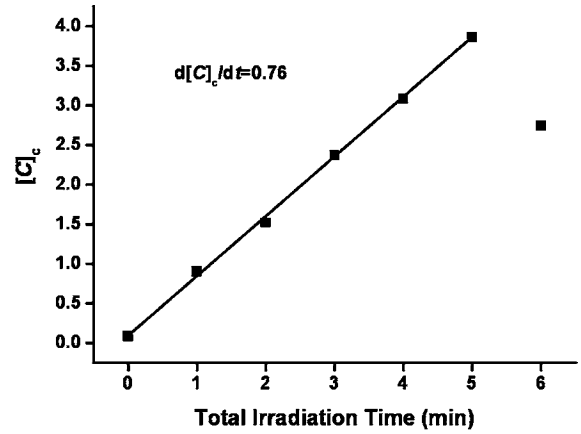

Figure 4. Plot of the concentration of FITC released from GNRs/FITC@PAA conjugates as a function of total irradiation time under the continuous irradiations.

Before laser exposure, the UV−vis absorption spectra of gold nanorods in the solution before the conjugation clearly exhibited two surface plasma absorption bands at ∼510 and ∼778 nm, corresponding to their transverse and longitudinal surface plasma bands, respectively. Slight red shifts (∼3 nm) were observed after gold nanorods were conjugated with polyelectrolytes in the transverse surface plasma band for GNRs/FITC@PAA and GNRs/PTX@PDC conjugates. In addition, the blue shift in the longitudinal surface plasma band of GNRs/FITC@PAA conjugates was calculated to be ∼11 nm. The red shift in the longitudinal surface plasma band of GNRs/PTX@PDC conjugates was calculated to be ∼42 nm. The shifts of surface plasma absorption bands of gold nanorods are attributed to the changes in the local refractive index from water to polyelectrolytes and the surface charge of gold nanorod conjugates after the embedding.[20,35,40] Furthermore, the decreasing ratio of the longitudinal surface plasma band to transverse surface plasma band intensity was calculated to be ∼1.52 for GNRs/FITC@PAA conjugates and ∼1.59 for GNRs/PTX@PDC conjugates, respectively, compared to the gold nanorods without polyelectrolytes conjugating (∼3.50). Moreover, the gold nanorod conjugates in the transverse and longitudinal surface plasma bands also showed a broadening peak. Regarding the longitudinal and transverse surface plasma bands, the decreasing ratio and the broadening peaks can be attributed to the gold nanorods embedded in gold nanorod conjugates.

After the laser exposure, the samples were examined by UV−vis spectroscopy and TEM. The UV−vis absorption spectra of gold nanorods and GNRs/FITC@PAA conjugates before and after laser irradiation were shown in Figure 3. All spectra clearly exhibited two surface plasma absorption bands, corresponding to the transverse and longitudinal surface plasma bands of gold nanorods. The shifts and broadening of the surface plasma bands of the gold nanorods conjugates were observed in comparison to those pure gold nanorods before the conjugation. The changes before and after the conjugation were mainly attributed to the differences of the local refractive indexes between water and polyelectrolyte relative to gold nanorods. No observable change was found in the UV−vis spectra and TEM images of the conjugates before and after the laser irradiation for 300 s at 1 W/cm^2 (not shown). The intensity decrease at ∼775 nm (Figure 3) was found in the spectrum of the conjugates after laser irradiation for 600 s at 1 W/cm^2. The decrease was mainly attributed to the melting of gold nanorods because of the photothermal effect.[48,49] When the laser power was increased to 1.9 W/cm^2 with 120 s irradiation time, the PAA of the conjugates was destroyed according to TEM measurements. In contrast, when the laser lower power was decreased to 0.7 W/cm^2 with 600 s irradiation time, no any structural change of the conjugates was observed and no release of FITC occurred. Overall, to explore the release kinetics of FITC below, we chose the irradiation conditions which include the laser power being maintained at 1 W/cm^2 and the irradiation time being controlled within 0−5 min. Under such experimental conditions, the release of FITC can be triggered under laser exposure and the amount of released FITC was controlled by the accumulated irradiation time. Also, no significant structural change of gold nanorods of the conjugates occurred after the irradiation so that the multiple release of FITC became feasible.

Release Kinetics of FITC from GNRs/FITC@PAA Conjugates by Continuous NIR Laser Irradiation. The release kinetics of FITC from GNRs/FITC@PAA conjugates under NIR laser irradiation was studied. Here, the fluorescent FITC molecules were treated as a model drug and released away from GNRs/FITC@PAA conjugates. Before the conjugation, the photostability of free FITC was tested first. No photobleaching of FTIC solution was observed after NIR laser irradiation for 30 min at the power setting 1 W/cm^2. Also, GNRs/FITC@PAA conjugates in 1 mM NaCl solution were placed in the air without blocking the room light for 24 h to test the stability of the conjugate under ambient conditions. The results showed that no precipitate was observed in the solution and no release of FITC from GNRs/FITC@PAA conjugates was found. Obviously, FITC molecules were stably embedded inside the PAA layer.

A simple experiment was designed to study the release kinetics of FITC from GNRs/FITC@PAA conjugates under NIR laser irradiation. First, six individual solutions of the conjugates with the same concentration were dispersed in 1 mM NaCl solution. Then, the six solutions were irradiated individually with the laser at the power setting 1 W/cm^2 for 1, 2, 3, ..., 6 min, respectively. After irradiation, the concentrations ($[C]_c$) of FITC released from the conjugates in each sample were recorded and plotted as a function of total irradiation time in Figure 4. Clearly, $[C]_c$ increased as t increased within 5 min and reached the maximum, $[C]_c = 3.76\ \mu$M, at $t = 5$ min. The release rate

(48) Link, S.; Burda, C.; Nikoobakht, B.; El-Sayed, M. A. *J. Phys. Chem. B* **2000**, *104*, 6152–6163.
(49) Link, S.; El-Sayed, M. A. *J. Phys. Chem. B* **1999**, *103*, 8410–8426.

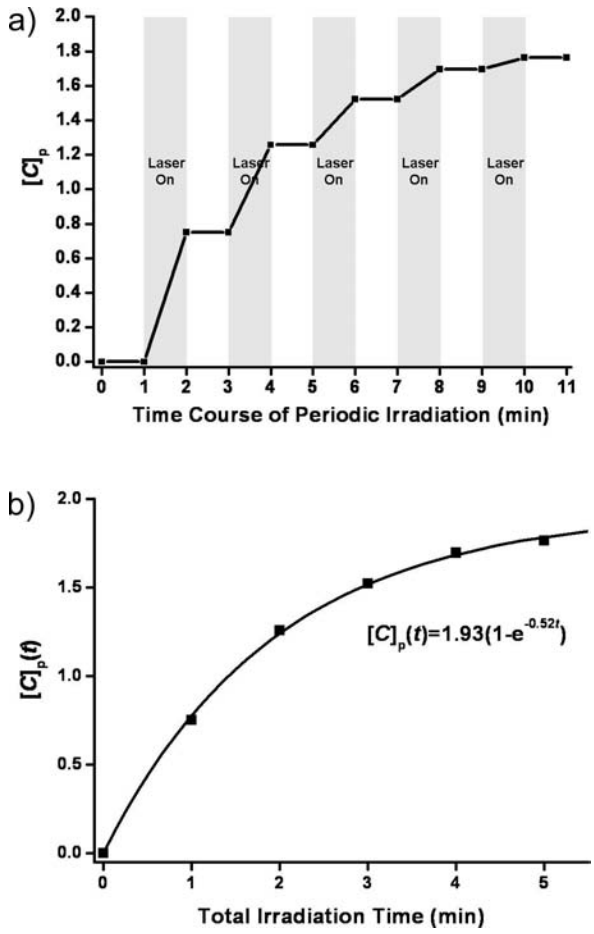

Figure 5. (a) Release profile of FITC when GNRs/FITC@PAA conjugates were periodically exposed under laser irradiation for 1 min with the interval of 1 min. Every strip bar in color represents the time period that the conjugates were under irradiation. The time period between the bars represents the interval without irradiation. (b) Plot of the concentration of FITC released from GNRs/FITC@PAA conjugates as a function of accumulated irradiation time under periodic laser irradiation. Here, $[C]_p(t)$ was obtained from the data in (a). The curve of $[C]_p(t)$ versus t was plotted based on first-order kinetics.

of FITC from GNRs/FITC@PAA conjugates was calculated to be nearly constant ($d[C]_c/dt = 0.76$, zero-order kinetics) within 5 min by continuous NIR laser irradiation. However, as t was over 5 min, $[C]_c$ dropped significantly due to the decomposition of the conjugates and thermal fluorescence quenching of released FITC. The decomposition and thermal quenching were very likely caused by the heat transferring from gold nanorods after a long period of laser irradiation. The overall results in Figure 4 suggested that the release of FITC was strongly correlated to the released heat from gold nanorods to the conjugates because of the photothermal effect.

Release Kinetics of FITC from GNRs/FITC@PAA Conjugates by Periodic NIR Laser Irradiation. To further understand the kinetics of FITC released from the conjugates, the concentration of released FITC was measured under periodic NIR laser irradiation. First, the conjugate solutions were prepared at the same concentration as those samples used above. The solution was then exposed periodically under the irradiation for 1 min following a 1 min interval, and the concentrations of released FITC were recorded within total 10 min time course. Then, the concentrations were plotted as a function of time course in Figure 5a. During the first 1 min irradiation, the release rate of FITC was nearly identical to that of the data in Figure 4. Afterward, during a 1 min nonirradiation interval, the concentration of released FITC remained unchanged, indicating that the release of FITC into the solution was stopped as soon as the laser was turned off. Then, FITC was released again from the conjugates during another 1 min irradiation period. As we can observe in Figure 5a, the augmentation in each 1 min irradiation period decreased with the increase of total irradiation time. Also, the concentration of released FITC remained constant during every nonirradiation intervals.

To understand the release kinetics of FITC by periodic irradiation, $[C]_p(t)$ (the concentration of released FITC after irradiation) was plotted versus t (total accumulated irradiation time) in Figure 5b. Here, $[C]_p(t)$ was obtained from the data in Figure 5a and t was increased from 1 to 5 min. Very interestingly, the data in Figure 5b exhibited completely different release kinetics in comparison to those in Figure 4. The curve of $[C]_p(t)$ versus t in Figure 5b was plotted based on the first-order kinetics:

$$[C]_p(t) = [C]_p(\infty)(1 - e^{-kt})$$

Here, we assumed that $[C]_p(\infty)$ is the maximum concentration of FITC released from the conjugates into the solution as the total laser irradiation time t goes to infinity and k is the release rate constant. The curve of $[C]_p(t)$ versus t showed an inverse exponential increase and reached the maximum $[C]_p(\infty) = 1.93$ μM, with the rate constant $k = 0.52$. The fitted line of first-order kinetics was the most appropriate one to describe the mechanism of FITC released from GNRs/FITC@PAA conjugates into the solution under periodic irradiation. The first-order release kinetics in this case was similar to that in most pharmacokinetics systems.[50−52] Notice that the maximum concentrations under continuous and periodic irradiations (Figures 4 and 5b) were 3.96 and 1.93 μM, respectively. The differences are explained based on the proposed release mechanism as described below.

Mechanism of FITC Released from GNRs/FITC@PAA under Laser Irradiation. A simple model was proposed to understand the mechanism of FITC released from GNRs/FITC@PAA conjugates under laser irradiation. Before laser irradiation, FITC molecules were conjugated well with PAA by the charge interaction between cationic FITC and anionic PAA. When the NIR laser is applied, the gold nanorods in GNRs/FITC@PAA conjugates can absorb the NIR laser and then photoenergy is transformed into heat by the photothermal effect. The heat is accumulated on the gold nanorods between 10 and 50 ps and is also dissipated to the surrounding approximately within 100 ps to 1 ns. Therefore, the temperature of the gold nanorods is raised under NIR laser irradiation. During the heat accumulation and dissipation process, the PAA of the conjugates is expanded and also the kinetic energy of the FITC of the conjugates is increased to be high enough to overcome the charge interaction.[53,54] As a result, FITC is released into the solution. Once the NIR laser is turned off, the heat from the gold nanorods of the conjugates is dissipated away within 100 ps to 1 ns. Within a very short time, the kinetic

(50) Jeong, B.; Bae, Y. H.; Kim, S. W. *J. Controlled Release* **2000**, *63*, 155–163.
(51) Wood, K. C.; Boedicker, J. Q.; Lynn, D. M.; Hammon, P. T. *Langmuir* **2005**, *21*, 1603–1609.
(52) Park, E. S.; Maniar, M.; Shah, J. C. *J. Controlled Release* **1998**, *52*, 179–189.
(53) Wei, C.; Srivastava, D.; Cho, K. *Nano Lett.* **2002**, *2*, 647–650.
(54) Rao, Y.; Blanton, T. N. *Macromolecules* **2008**, *41*, 935–941.

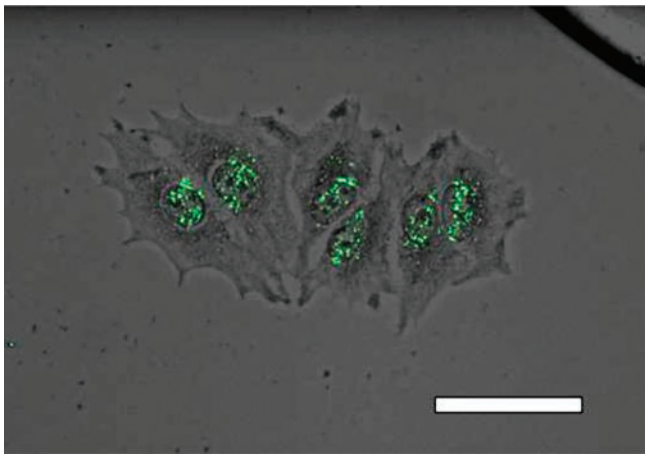

Figure 6. Two-dimensional confocal microscopic image of MCF-7 cells incubated with GNRs@FITC/PAA conjugates (green color). The cross section image confirms that the conjugates are located inside the cells. The scale bar is 50 μm.

energy of FITC is too low to overcome the charge interaction and the release of FITC is suppressed immediately.

The differences in the release kinetics of FITC in Figures 4 and 5b ($[C]_c(t)$ and $[C]_p(t)$ versus t) can be understood based on our proposed model above. Within the 5 min irradiation period, the release rate of FITC remained constant under continuous irradiation (Figure 4); in contrast, the release rate was decreased with the first-order kinetics under periodic irradiation (Figure 5b). When the accumulated irradiation time was increased, the total FITC molecules with enough kinetic energy to escape from the conjugates into the solution were increased. Therefore, the release rate of FITC was kept a constant in 5 min continuous irradiation period. However, after each one-min irradiation and then one min interval, the accumulated heat from laser irradiation was dissipated away during the interval. So, with a limited amount of FITC, the total FITC molecules with enough kinetic energy were decreased after each one min irradiation. As a result, the release rate of FITC showed first-order kinetic behavior similar to most drug release kinetics in biocompatible polymer based systems. In those systems, drugs such as ketoprofen, cefazolin, bupivacaine, and taxol released from hydrogel demonstrated a first-order release profile.[48−50] The data in Figure 4 and Figure 5b also showed that the maximum concentrations of released FITC were 3.76 and 1.93 μM, respectively. The results agreed with the model that the release of FITC away from the conjugates mainly was caused by the heat transferred from the gold nanorods under laser irradiation. With a longer irradiation time, the total number of FITC molecules that can escape from the conjugates was expected to be higher (Figure 4).

Fluorescence Image of GNRs/FITC@PAA Conjugates in Cells Using Confocal Microscopy. We further investigated whether the GNRs/FITC@PAA conjugates can be utilized in living cells as a carrier for drug delivery. In drug delivery systems, most drug carriers must be successfully internalized into cells and then the drugs were released from the carriers in order to achieve the best therapeutic effect. Here, the fluorescence of the FITC molecules of the GNRs/FITC@PAA conjugates was monitored under a confocal microscope after the conjugates were incubated with MCF-7 cells. The strong green fluorescence of FITC was clearly observed inside the cells as shown in Figure 6. The image indicated that the conjugates were mainly located near the center of cell nuclei. Several reports have indicated that the nanomaterials such as quantum dots and carbon nanotubes have entered mammalian cells through endocytosis.[55−60] On the basis of our observation under the microscope, we also believed that GNRs/FITC@PAA conjugates have entered the cells through endocytosis. After the cells irradiated with the laser, the strong green fluorescence of FITC was still observed near the cell nuclei, indicating that the released FITC from the conjugates was not randomly distributed in the entire cell. The result might be attributed to the reaction of FITC with the amine group in the nuclear proteins.[61−63]

Cell Viability Assay of GNRs/PTX@PDC Conjugates Incubated with MCF-7 Breast Cancer. Anticancer drug PTX has demonstrated clinical activity in breast cancer because it can lead to the apoptosis of the cancer cells by preventing microtubule depolymerization. The location of breast cancer is usually near the epidermis where an NIR laser in the 800−1100 nm region can penetrate. On the basis of our studies on the release kinetics of FITC above, the design of a new effective anticancer drug delivery system becomes feasible providing that PTX can successfully be delivered and then preciously released near breast cancer cells by laser irradiation. Here, we chose PTX as the delivered drug. The GNRs/PTX@PDC conjugates were prepared, and an investigation of the release of PTX to inhibit cancer cell growth was performed using NIR laser irradiation as a release trigger.

The control experiment was first performed to test the cytotoxicity of free gold nanorods and gold nanorod conjugates. After the cells were incubated individually with gold nanorod samples with a certain concentration for 12−24 h,[64] in vitro cell viability was analyzed by an MTT assay. The viability of MCF-7 cells treated by GNRs/PTX@PDC conjugates, GNRs@PAA/PDC conjugates, and gold nanorods was found to be 81%, 82%, and 87%, respectively. The high viability of the cells indicated that all three samples did not generate much cytotoxicity after they entered the cells. Therefore, we chose the concentrations in the experiment to execute the inhibition rate measurements under laser irradiation below. However, when the concentrations of each conjugates and the gold nanorods were increased by 10 times, we found that the cell viability of MCF-7 cells was reduced to 42%, 46% and 50%, respectively.

Inhibition Rates of GNRs/PTX@PDC Conjugates for MCF-7 Breast Cancer Cells after NIR Laser Irradiation. To study the release of PTX from GNRs/PTX@PDC conjugates under laser

(55) Dubertret, B.; Skourides, P.; Norris, D. J.; Noireaux, V.; Brivanlou, A. H.; Libchaber, A. *Science* **2002**, *298*, 1759–1762.
(56) Bruchez, M.; Moronne, M.; Gin, P.; Weiss, S.; Alivisatos, A. P. *Science* **1998**, *281*, 2013–2016.
(57) Kam, N. W. S.; Dai, H. J. *J. Am. Chem. Soc.* **2005**, *127*, 6021–6026.
(58) Kam, N. W. S.; Jessop, T. C.; Wender, P. A.; Dai, H. J. *J. Am. Chem. Soc.* **2004**, *126*, 6850–6851.
(59) Nakayama-Ratchford, N.; Bangsaruntip, S.; Sun, X. M.; Welsher, K.; Dai, H. J. *J. Am. Chem. Soc.* **2007**, *129*, 2448–2449.
(60) Chan, W. C. W.; Nie, S. M. *Science* **1998**, *281*, 2016–2018.
(61) Lin, C. C.; Anseth, K. S. *Adv. Funct. Mater.* **2009**, *19*, 2325–2331.
(62) Hubmacher, D.; Tiedemann, K.; Bartels, R.; Brinckmann, J.; Vollbrandt, T.; Batge, B.; Notbohm, H.; Reinhardt, D. P. *J. Biol. Chem.* **2005**, *280*, 34946–34955.
(63) Handman, E.; Remington, J. S. *Infect. Immun.* **1980**, *29*, 215–220.
(64) For our laser irradiation experiments, a titanium-sapphire laser tuned to a wavelength of 775 nm was used to irradiate gold nanorod conjugates. Therefore, we calibrated the concentrations of gold nanorod conjugate solutions by measuring the intensity of optical absorption of gold nanorods at 775 nm using a UV−vis spectrometer. In the cell viability and inhibition experiments of this work, the concentrations of GNRs/PTX@PDC conjugates, GNRs@PAA/PDC conjugates, and gold nanorod solutions were maintained at the absorption intensity of 0.07 at 775 nm.

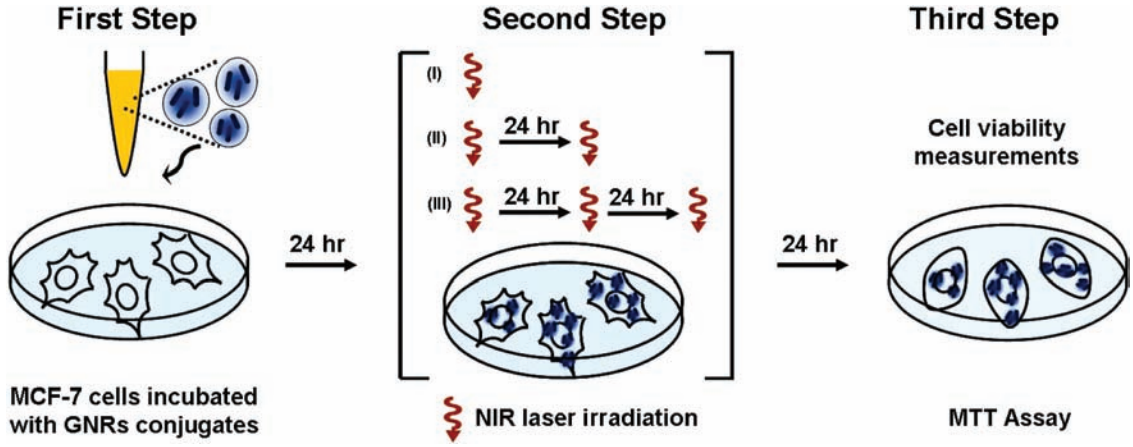

Figure 7. Schematic illustration of the experimental procedures to measure the cell viability of MCF-7 cells with GNRs/PTX@PDC conjugates inside after laser irradiation. There were three major steps in the experiment. In the first step, MCF-7 cells were incubated with GNRs/PTX@PDC conjugates for 24 h. Then, in the second step, the cells with the conjugates inside were irradiated by the NIR laser with the irradiation mode (I), (II), or (III). In the irradiation mode (I), NIR laser was applied continuously for 20, 40, 60, or 120 s. In the irradiation modes (II) and (III), NIR was applied periodically in either two laser exposures or three laser exposures. Between each laser exposure, the cells were subsequently cultured for 24 h. Finally, in the third step, the cell viability of the irradiated MCF-7 cells was measured with an MTT assay, and then the inhibition rate of the cells was calculated.

irradiation, we have designed a series of experiments and described the detailed steps in Figure 7. In the first step, MCF-7 cells were incubated with GNRs/PTX@PDC conjugates for 24 h to ensure that the conjugates can successfully enter the cells through endocytosis. Then, in the second step, the cells with the conjugates inside were irradiated by an NIR laser in either a continuous or periodic irradiation mode for different irradiation periods. Finally, in the third step, the irradiated MCF-7 cells were cultured for an additional 24 h. At this stage, the viability of the irradiated cells was carefully evaluated by the MTT assay and also the inhibition rate was calculated based on the following:

$$\text{Inhibition rate}(\%) = \frac{OD_{570}(w/o\ laser) - OD_{570}(with\ laser)}{OD_{570}(w/o\ laser)} x100\%$$

Here, OD_{570} (*w/o laser*) and OD_{570} (*with laser*) are the absorbance at 570 nm using the MTT assay after the MCF-7 cells were treated with GNRs/PTX@PDC conjugates and then irradiated without (*w/o*) and with the NIR laser, respectively.[65,66]

The inhibition rates of the cells with GNRs/PTX@PDC conjugates were evaluated after the irradiation modes (I), (II), and (III) were applied for various time periods. The experimental steps of each irradiation mode and abbreviation below were described in Figure 7. First, irradiation modes (I)-20, -40, -60, and -120 were executed to the individual cell samples and then the inhibition rates of the cell were measured. Here, (I) and -number represent one laser shot and the irradiation time (in seconds) of the shot, respectively. The inhibition rates versus accumulated irradiation times were plotted in Figure 8. The results showed that the inhibition rates were increased significantly from 8.5 to 25.9% with increases of the total irradiation times from 20 to 120 s, respectively.

The inhibition rates of the cells were also measured after irradiation modes (II)-60/60, (II)-120/120, (III)-60/60/60, and (III)-120/120/120 were applied to the individual cell samples. Here, (II) and (III) represent two shots and three shots of laser irradiation, respectively, and -number/number stands for the irradiation time (in seconds) of each shot (Figure 7). After all the experimental steps were completed, the inhibition rates versus the total accumulated irradiation time were plotted in Figure 8. Clear differences in the inhibition rates were found after irradiation modes (I)-60, (II)-60/60, (III)-60/60/60, (I)-120, (II)-120/120, and (III)-120/120/120 were individually applied to the MCF-7 cells. The results indicated that the inhibition rates were increased with increases in total irradiation time in both continuous and periodic irradiation modes. Also, with the increases of each laser shot (either 60 or 120 s), the significant increases of the inhibition rates were measured. In contrast, the inhibition rates remained unchanged without the additional shot after a 24 h culture.

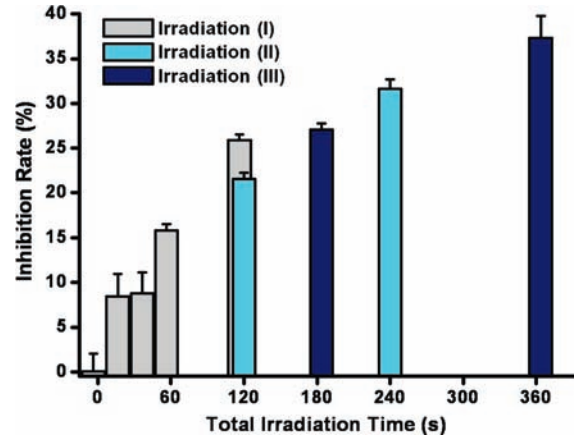

Figure 8. Inhibition rates of MCF cells with GNRs/PTX@PDC inside were calculated based on the viability of the cells after the irradiation modes (I), (II), and (III) were applied onto cells individually. The accumulated irradiation time of irradiation modes (II) and (III) was obtained from the sum of each irradiation period. The inhibition rate of the cells at the accumulated irradiation time = 0 was obtained from the controlled experiment and defined as zero.

In Figure 8, with the same accumulated irradiation time (120 s), the inhibition rates of MCF-7 cells were found to be 25.9 and 21.6% after the laser irradiation of modes (I)-120 and (II)-60/60 was applied, respectively. The release mechanism of PTX

(65) Wu, Y.; Shen, D.; Chen, Z.; Clayton, S.; Vadgama, J. V. *Apoptosis* **2007**, *12*, 593–612.
(66) Hahn, S. M.; Liebmann, J. E.; Cook, J.; Fisher, J.; Goldspiel, B.; Venzon, D.; Mitchell, J. B.; Kaufman, D. *Cancer* **1993**, *72*, 2705–2711.

from GNRs/PTX@PDC conjugates was expected to be similar to that of FITC from GNRs/FITC@PAA conjugates. The different inhibition rates probably were due to the different concentrations of released PTX in the cells. In the continuous irradiation mode, (I)-120, the extent of heat accumulation on gold nanorod conjugates was expected to be higher than that in the periodic irradiation modes, (I)-60/60. During the interval between each laser shot with the irradiation mode (II)-60/60, the accumulated heat was dissipated away very fast in comparison to the case with the irradiation mode (I)-120. On the basis of the current results, we expect that the concentration of released PTX should be able to be adjusted by variation of the laser irradiation time and modes.

To further confirm the origins of the inhibition of the cell growth, we also performed control experiments on MCF-7 cells with GNRs/PAA@PDC conjugates (notice that no anticancer drug, PTX, was inside the conjugates). First, the conjugates were incubated with the MCF-7 cells, and then, the cells were irradiated individually by the NIR laser using irradiation modes (I), (II), and (III) (also see Figure 7 for detailed experimental steps). All results showed that the inhibition rates of the cells were approximately zero, indicating that the cell viability was not affected by laser irradiation and that the inhibition of the cell growth was very likely caused by the releases of PTX into the cells.

The results in Figure 8 have indicated that the inhibition rates were increased when the total irradiation time was increased. We expected that the release mechanism of PTX from GNRs/PTX@PDC conjugates was similar to that of FITC released from the GNRs/FITC@PAA conjugates under laser irradiation. When the NIR laser was executed, gold nanorods in GNRs/PTX@PDC conjugates can absorb NIR irradiation and then the photoenergy is transformed into heat by the photothermal effect. During heat accumulation and dissipation, the PDC of the conjugates was expanded and also the kinetic energy of PTX near the gold nanorods of the conjugates was increased enough to overcome the charge interaction. As a result, PTX was released. Therefore, when the total irradiation time was increased, the amount of PTX with enough kinetic energy to escape from the conjugates into the solution was increased.

The GNRs/PTX@PDC conjugates exhibited quite different release kinetics by laser irradiation in comparison to the conventional PTX capsules of PTX-loaded polymeric nanoparticles. In general, the in vitro release of PTX from the polymeric nanoparticles was fast in the first 4 h. After the initial burst of release, the release rate of PTX slowed down and became an almost zero-order rate of release.[67−70] During the first 24 h, the inhibition rate of cell lines incubated with conventional polymeric nanoparticles was observed to reach the maximum. Also, after cell line incubation with polymeric nanoparticles for 48−72 h, the inhibition rates of cell lines were gradually increased. In our system, by the selection of the irradiation modes and time, the release of PTX from GNRs/PTX@PDC conjugates could be well controlled even after the conjugates remained with MCF-7 cells for 96 h. Currently, the continuous studies of our new PTX release system were performed in vitro and in vivo in order to reach maximum therapeutics for breast cancers.

Conclusions

In conclusion, the kinetic behaviors of FITC released from GNRs/FITC@PLE conjugates were studied under NIR laser irradiation. Within 5 min of accumulated irradiation, the release rates of FITC showed zero- and first-order kinetics under continuous and periodic irradiations, respectively. The inhibition rates of breast cancer cells were studied after GNRs/PTX@PLE conjugates were incubated with the cells and then irradiated with the laser. The inhibition rates showed a clear dependency on the laser irradiation modes and time. The results suggested that the multiple release of the anticancer drug from the conjugates became feasible by laser irradiation within a long period of time. Overall, our studies have showed a new route for therapeutic applications on breast cancer cells in the near future.

Acknowledgment. This work was supported by NSC-98-3114-M-003-001, TNSTPNN, IAMS, and NTNU.

JA105360Z

(67) Lee, A. L. Z.; Wang, Y.; Cheng, H. Y.; Pervaiz, S.; Yang, Y. Y. *Biomaterials* **2009**, *30*, 919–927.
(68) Danhier, F.; Magotteaux, N.; Ucakar, B.; Lecouturier, N.; Brewster, M.; Preat, V. *Eur. J. Pharm. Biopharm.* **2009**, *73*, 230–238.
(69) Danhier, F.; Lecouturier, N.; Vroman, B.; Jerome, C.; Marchand-Brynaert, J.; Feron, O.; Preat, V. *J. Controlled Release* **2009**, *133*, 11–17.
(70) Seowa, W. Y.; Xuea, J. M.; Yang, Y. Y. *Biomaterials* **2007**, *28*, 1730–1740.